

Manufacturing Letters

Manufacturing Letters 00 (2023) 000-000



51st SME North American Manufacturing Research Conference (NAMRC 51, 2023)

Missing Signal Imputation for Multi-channel Sensing Signals on Rotary Machinery by Tensor Factorization

Abdullah Al Mamun a, Mahathir Mohammad Bappy a, Linkan Bian a, b Sara Fuller b, TC Falls c, and Wenmeng Tian a,b*

- ^a Department of Industrial and Systems Engineering, Mississippi State University, Mississippi State, MS 39762, USA
 - ^b Center for Advanced Vehicular Systems, Mississippi State University, Mississippi State, MS 39762, USA
 - ^c Institute for Systems Engineering Research, Mississippi State University, Vicksburg, MS 39180, USA * Corresponding author. Tel.: +1 662.325.9220; fax: +1 662.325.7618. E-mail address: tian@ise.msstate.edu

Abstract

Multi-channel sensor fusion can be challenging for real-time machinery fault identification and diagnosis when a substantial amount of missing data exists. Usually, some (or even all) sensors may not function correctly during real-time data acquisition due to sensor malfunction or transmission issues. Additionally, multi-channel sensor fusion yields a large volume of data. Imputation of missing entries can also be challenging with a large volume of data, which can predominantly affect the accuracy of machinery fault diagnosis. However, how to impute a substantial amount of missing data for machinery fault identification is an open research question. In light of the above challenges, this paper proposes constructing time-domain tensors based on heterogeneous sensor signals. Subsequently, the fully Bayesian CANDECOMP/PARAFAC (FBCP) factorization method is adopted for missing data imputation of diverse bearing faults signals. To validate the effectiveness of this proposed method, a machinery fault simulator was used to collect diverse bearing fault signals by incorporating both acoustics and vibration sensors. A varying percentage of continuous missing signal scenarios are introduced at the random locations among different acoustics and vibration channels to construct incomplete tensors. Subsequently, the FBCP method was leveraged to complete the incomplete tensors and calculate estimated tensors. To evaluate the performance of continuous missing data imputation, relative standard errors are computed based on the estimated and actual time-domain tensors. Experimental results show that this proposed method can effectively impute a substantial portion of continuous missing data from diverse bearing fault scenarios.

© 2023 Society of Manufacturing Engineers (SME). Published by Elsevier Ltd. All rights reserved. This is an open access article under the CC BY-NC-ND license (http://creativecommons.org/licenses/by-nc-nd/4.0/) Peer-review under responsibility of the Scientific Committee of the NAMRI/SME.

Keywords: Acoustics and vibration signals; condition monitoring; fault diagnosis; missing data imputation; sensor fusion; tensor completion.

1. Introduction

1.1. Motivation and challenges

Advanced communication and sensing technologies have established the platforms between the physical manufacturing plants and the cyber world, which is defined as cyber-physical manufacturing systems [1]. In cyber-physical systems, a manufacturing plant can be operated and monitored simultaneously at the physical plants with the help of remotely controlled sensors that can collect real-time data for process

monitoring and decision-making [2]–[4]. The emerging trend of multi-channel sensor fusion is ubiquitous. Industry 4.0 perspective, heterogeneous sensor fusion can be integrated real-time for condition monitoring of machinery [5]. Advanced sensing technologies provide novel opportunities for real-time fault diagnosis of manufacturing machinery. Different sensors, including accelerometers, infrared imaging sensors, microphones, power loggers, and thermocouples, are widely used for collecting real-time sensing signals[6], [7]. Among those sensing technologies, microphones and accelerometers are extensively used for acoustic and vibration signals.

Numerous studies showed that combining acoustics and vibration signals is more effective than the individual signal analysis approach [8], [9]

Generally, multi-channel sensor fusion yields a large volume of data. Hence, efficient sensor performance and real-time data acquisition is significantly important for machinery prognostics and health management (PHM) task [3]. However, signal missing may prevail due to various reasons, including sensor sensitivity malfunction, sensor hardware malfunction, and transmission disruptions [10]-[13]. The effect of signal missing data may ends up with either continuous or random missing data [10]. Moreover, in the worst-case scenarios, for example, during a blackout situation, a substantial portion of continuous missing data may also occur [14], [15]. Ultimately, this leads to a substantial volume of missing data occurrence. While imputation of missing entries can also be challenging, and that can also predominantly affect the performance of imputation. However, the multidimensional data structure, which is defined as a tensor, provides an effective way to handle high-volume of data. Tensor completion task with substantially missing data volume effectively imputes missing entries when sensor signal missing occurrence exists. Additionally, tensor factorization enables to capture of multilinear interaction (channels × signals) among latent factors of sensor signals and imputes missing entries based on observed signals [15], [16].

Seeking state-of-the-art, a significant number of studies have been involved in imputing missing entries by adopting tensor completion. This study has incorporated CANDECOMP/PARAFAC (CP) tensor factorizations method that captures multi-linear structures and incomplete tensor completion tasks. This study adopted a tensorial missing signal imputation by a fully Bayesian CANDECOMP/PARAFAC (FBCP) factorization method with low-rank determination [16]. The FBCP method provides several competitive advantages in dealing with missing signal imputation along with incomplete tensor completion. For instance, a. FBCP method can automatically determine CP rank, b. efficiently avoid overfitting, c. performs well in imputing missing entries with incomplete tensors.

1.2. Technical contribution of this proposed method

This proposed method was conducted on a machinery faults simulator (MFS) based on different bearing fault scenarios by incorporating acoustics and vibration signals. A varying percentage of continuous missing signal scenarios is generated among an equal number of acoustics and vibration channels with a unified length of signals. And then constructed timedomain tensor. Missing signal imputation in the time-domain tensor was adopted by a FBCP factorization method [16]. Fig. 1 demonstrates continuous missing signals among different channels. It is worth noting that a continuous missing entry is introduced at a random location with varying missing percent based on a given length of signals.

 The FBCP method enables to capture of multi-linear interaction (channels × signals) among latent factors of sensor signals.

- The FBCP method performs missing entries imputation along with incomplete tensor completion with low-rank determination.
- Overall, this proposed method performed well imputing a varying length of continuous missing entries of multichannel sensor signals from diverse bearing fault conditions.

2. Literature review

A systematic state-of-the-art has been conducted based on mechanisms of missing data and different imputation methods. Section 2.1 primarily demonstrated the mechanisms of missing data and types of missing data patterns. In section 2.2, missing data imputation mechanisms are briefly discussed. A summary of the research gap is demonstrated in section 2.3.

2.1. Missing data patterns and their generating mechanisms

Missing data problems are widespread in various applications, including industrial, social, biomedical, and weather science [17]–[19]. Missing data pattern describes the structure between missing entries and observed datasets. Missing data mechanisms refer to probable relations between the given variables and missing data [17]. Usually identifying the cause of missing data is usually somewhat difficult, but some inferences can help detect the missing data pattern [20]. Missing data occurrence can be responsible for various reasons, including sensor failure, sensor aging, hardware malfunction, and transmission interference [10]–[13].

Missing data mechanism can be explained by three mutually exclusive categories: a. missing at random (MAR); b. missing completely at random (MCAR); c. missing not at random (MNAR) [17], [20], [21]. MAR relates the systematic link between one or more calculate variables and the probability of missing data [17], [22]. MAR occurrence is not random and explains the systematic missing. Additionally, MAR also explains the tendency for missing data that are correlated with associated variables [22]. MAR may occur due to transmission interruption that may end up with continuous missing signals [10]. For example, in a global navigation satellite system, time series data can be missing as MAR due to receiver crashes and power failure [23]–[25]. Offshore wind farms face difficulties of supervisory control and data acquisition systems when signals are missing due to harsh weather condition that led to sensor failure [26], [27]. MAR occurrence can also be found in wireless sensor networks due to sensor's node communication lost [28]. MCAR occurrence is completely haphazard, and the observed data can be assumed a random subsample of the complete data. The probability of MCAR data is unrelated of a given variable and also unrelated to other variables [22]. In contrast with MAR, MCAR data follow more restrictive conditions because of missing data is completely unrelated to the data [17], [22]. For instance, Micro-electromechanical systems (MEMS) senor malfunctioning can also be explained by MCAR behavior based on its functional level that relates to several factors such as thermomechanical failure, electrical failure, and environmental failure [29]. Sound signal loss is also associated with MCAR due to malfunctioning microphone's electro-acoustic sensitivity [30], [31]. MNAR exists when the probability of missing data on a given variable

is related to the value of itself. While other variables can also be controlled. MNAR is likely to be related to unobserved data. Similar to the MAR mechanism, there is no straightforward way to confirm that records are MNAR without observing the entries of the missing variables [17].

2.2. Missing data imputation methods

Missing value recovery can be completed by different imputation techniques, including mean substitution that is replace by column mean or median [32]. K- nearest neighbor (KNN) is a widely used popular technique for missing data imputation [33], [34]. For example, KNN-based missing data imputation is implemented in wireless sensor networks missing sensor data [28]. Studies found that KNN performs better using continuous and discrete data [35]. However, the KNN-based imputation approach is time intensive since it searches for similar data patterns from its neighbors [36]. Different regression models, including multiple linear regression, logistics regression, and multinomial logistics regression, are used for missing data imputation [32]. Regression models establish a relation between missing and existing features, where existing features are defined as predictors. However, this regression shows poor performance when it cannot correlate missing and existing features [32], [37]. Fuzzy c-means clustering techniques applied for missing data imputation that seeks the related features of a missing feature, and multiple linear regression and support vector regression are utilized for the particular features from fuzzy cluster [18]. While this proposed method failed to select automatic parameter selection in the regression model. In the state-of-the-art, deep learning models are widely used in the missing data imputation approach. Artificial neural network (ANN) is also a popular method for missing data imputation [19], [27]. Overfitting occurrences can be found in ANN when it shows good performance in the training dataset but fails to perform better in the testing dataset [27]. In the biomedical field, the missing data imputation approach is also popular by using recurrent neural network (RNN) [38], [39]. RNN showed better performance on missing pattern prediction. In [38] method, the proposed model was restricted to explain the correlation between missing pattern and prediction task. Compressed Sensing -based on missing data imputation is utilized to condition monitoring of wind turbines [40]. However, Compressed Sensing-based on missing data imputation computational time is substantially high [41], [42].

Tensor completion methods are also widely used for high-dimensional missing data imputation. Tensor completion tasks can be categorized into several approaches, including decomposition/factorization-based, trace-norm based, and some other probabilistic methods. Tensor factorization coupled with tensor completion task is aligned to underlying factors based on partially observed data, and incorporating a multilinear generative model assumption with fixed rank enables the prediction of missing entries [16], [43], [44]. Most widely used tensor decomposition approach includes CANDECOMP/PARAFAC and Tucker decomposition [45]—[49]. Tensor factorization with missing data has been conducted with several approaches including weighted least square problem termed as CP weighted optimization

(CPWOPT) [50], CP with nonlinear squares (CPNLS) [51], geometric nonlinear conjugate gradient (geomCG) [52]. Still, the tensor factorization shows the tendency of overfitting because of incorrect tensor rank approximation and estimations of underlying factors that lead to poor predictive performance [16]. In contrast, significant research work has also been conducted missing data imputation based on low-rank tensor completion (LRTC) [16]. Musialski et al. [53] incorporated Gaussian residual-based expectation maximization (EM) approach in Tucker decomposition with smoothing scheme coupled with fast low rank tensor completion (FaLRTC) and high accuracy low rank tensor completion (HaLRTC). Certain probabilistic CP decomposition techniques with Bayesian inference are also suggested for resolving missing entries estimation problem. This method is based on log-likelihood function that deletes the missing values from likelihood functions to deal with missing values and perform imputation [54]. However, tensor rank minimization based on nuclear norm relies on parameter tuning approach, which performs over or under-estimating the true tensor rank. Tensor rank determination considers NP-complete because there is no simple algorithm for computer rank even with a given specific tensor [55]. Seeking the state-of-the-art solution, we have adopted a FBCP factorization with low-rank determination method for missing data imputation from a machinery faults simulator (MFS) with diverse bearing faults signals.

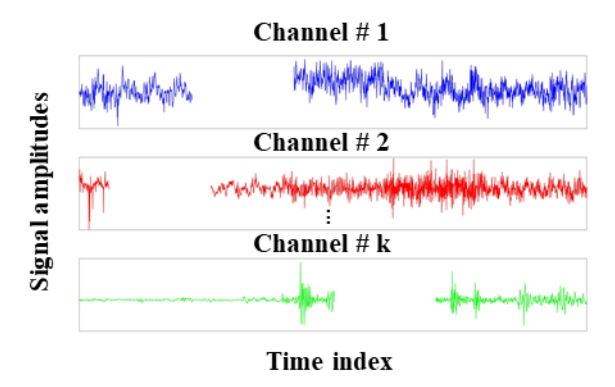


Fig. 1. Continuous missing of signals among different channels.

2.3. Summary of research gaps

After the systematic literature review, existing research gaps and challenges are identified, emphasizing missing data imputation by general, deep learning, and tensor completion methods in Table 1.

Table 1. Summary of existing research gap.

Missing data imputation method	C 1		
General method	 KNN approach is time intensive since it search for similar data pattern from its neighbours [36]. Multiple linear regression method shows poor performance when it cannot correlate missing and existing features [32], [37]. Fuzzy c-means clustering approach failed to select automatic parameter selection in the regression model [18]. 		

Deep Learning method	ANN approach shows good performance in training dataset but fails to perform better in testing dataset [27]. RNN model is restricted to explain the correlation between missing pattern and prediction task [38].	
Tensor Completion method	CPWOPT, CPNLS, and geomCG methods sethe tendency of overfitting because of incorn tensor rank approximation and estimations of underlying factors that lead to poor predictive performance[16], [50]–[52]. Tensor rank minimization on nuclear norm relies on tuning parameters, which could show over or under-estimating the true tensor rank [55].	

3. Methodology

In this section, the proposed method is presented to impute missing entries in the time-domain signals generated from acoustic and vibration sensors. A varying percentage of continuous missing signal scenarios is generated at a specific channel with a unified length of signals at random location of signals. And then constructed time-domain tensors with all channels at a time, which is defined as incomplete time-domain tensors. Missing signal imputation in incomplete time-domain tensor is adopted by a FBCP factorization method [16] and computed an estimated tensors. Thus, the performance evaluation of FBCP method is calculated based on relative standard error (RSE) of estimated and actual tensors. The overview of the proposed method is depicted in Fig. 2, which illustrates continuous missing signal scenarios at channel 1 and constructed incomplete time-domain tensors with all channels.

3.1. Tensor formation of the time-domain signal

Acoustics and vibration time-domain channel-wise signals are combined and expressed as $s_l^1(t)$, $s_l^2(t)$, $s_l^3(t)$, ..., $s_l^k(t)$, where k represents the total number of channels and l denotes the observation index as l = 1, 2, 3, ..., m. The combined time-domain signals with l observations are constructed as a time-

domain tensor with the dimension of $D \times k$. The resulting time-domain tensor contains the actual acoustics and vibration signals, which is denoted as $\mathcal{X}_{\Omega}(l) \in \mathbb{R}^{D \times k}$, where D represents the length of the unified time-domain signals, where channel-wise continuous missing signals can occur at random location. Furthermore, Ω denotes the set of indices in $\mathcal{X}_{\Omega}(l)$, and $(i_1,i_2) \in \Omega$ where $i_n=1,2,\ldots,I_n$, $I_1=D$ and $I_2=k$. With continuous missing entries in the signal, the incomplete time-domain tensor can be expressed as $\mathcal{X}'_{\Omega}(l) \in \mathbb{R}^{D \times k}$ (Fig. 2).

3.2. Bayesian-CP based tensor completion

The FBCP algorithm can effectively correlate the latent multi-linear factors based on the observed data with a low-rank determination and estimates the predictive distributions among missing entries. In this section, for simplicity, the sample index l of $\mathcal{X}_{\Omega}(l)$ is omitted, since the tensor completion is implemented on each individual sample separately. Let $\mathcal{X}'_{\Omega} \in \mathbb{R}^{D \times k}$ as a 2^{nd} -order tensor of dimension $D \times k$ with missing entries. The entries of $\mathcal{X}'_{\Omega} \in \mathbb{R}^{D \times k}$ can be denoted by \mathcal{X}'_{l_1, l_2} . The underlying idea of applying Bayesian-CP decomposition is to approximate the \mathcal{X}'_{Ω} , by generating the low-rank structure as shown in the Eq.(1) [56], $\widetilde{\mathcal{X}}'_{\Omega}$ is the estimated tensor.

$$\widetilde{\mathcal{X}}'_{\Omega} = \sum_{r=1}^{R} \mathbf{x}_{r}^{(1)} \, \mathbf{o} \, \, \mathbf{x}_{r}^{(2)} = \, [\![\mathbf{X}^{(1)}, \, \mathbf{X}^{(2)}]\!]$$
 (1)

where the operator o denotes the outer product of vectors, and [...] is termed as the Kruskal operator. The CP factorization can be calculated as a sum of R rank-one tensors, where the lowest integer R is determined as the CP rank [57]. $\{\mathbf{X}^{(n)}\}_{n=1}^2$ contains the set of n-th decomposed factor matrices, and $\mathbf{X}^{(n)} \in \mathbb{R}^{(D \times k) \times R}$ can be denoted as row-wise or column-wise vectors $\mathbf{X}^{(n)} = [\mathbf{x}_1^{(n)}, \dots \mathbf{x}_{i_n}^{(n)}, \dots, \mathbf{x}_{I_n}^{(n)}]^T = [\mathbf{x}_1^{(n)}, \dots \mathbf{x}_r^{(n)}, \dots, \mathbf{x}_R^{(n)}]$. The calculation of $\mathrm{Rank}_{CP}(\mathcal{X}_{\Omega}^r) = R$ is computationally challenging and costly. The Bayesian inference process can reach automatic low-rank approximation based on tensor factorization to avoid the overfitting problem. The CP generative missing entries assumption is based on

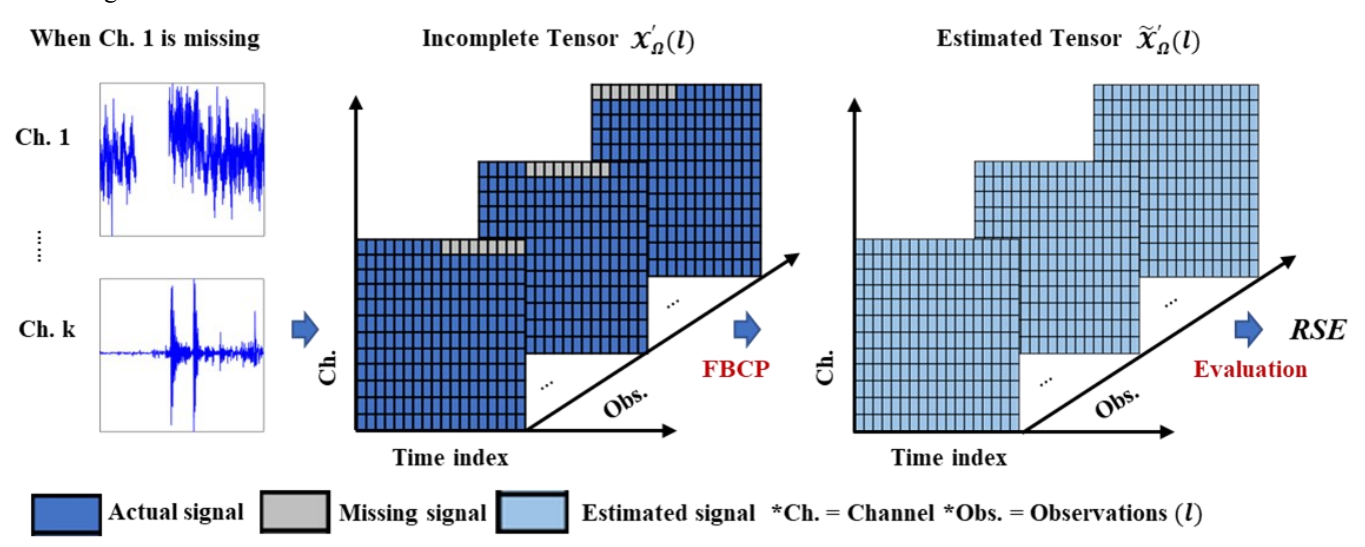


Fig. 2. The proposed framework for multi-channel missing signal imputation.

observed entries of \mathcal{X}'_{Ω} and the factorized tensor elements of $p(\mathcal{X}'_{\Omega}|\mathbf{X}^{(n)})$. Now, in order to enable automated rank determination, a sparsity-inducing prior is provided across the hyperparameters, since the smallest R is more desirable in low rank approximation. Specifically, the prior distribution over the latent factor can be determined by $\lambda = [\lambda_1, \dots, \lambda_R]$, where λ_r control r-th components in $\mathbf{X}^{(n)}$ that is expressed in the Eq. (2).

$$p(\mathbf{X}^{(n)}|\boldsymbol{\lambda}) = \prod_{i_n=1}^{l_n} \mathcal{N}(\mathbf{x}_r^{(n)}|0,\boldsymbol{\Lambda}^{-1}), n = 1,2$$
 (2)

where $\Lambda = \operatorname{diag}(\lambda)$ represents the inverse covariance matrix, also known as the precision matrix, that is shared from the latent factor matrix in all modes. The hyperprior over $p(\lambda)$ is a factorized dimension and characterized using a Gamma distribution. The latent variables and hyperparameters are collectively denoted in Eq. (3).

$$\Theta = \{\mathbf{X}^{(1)}, \mathbf{X}^{(2)}, \boldsymbol{\lambda}\} \tag{3}$$

The Bayesian computation of the full posterior distribution of all variables is demonstrated in the Eq. (4). Based on the posterior distribution of all variables in Θ , the predictive distribution of missing entries is estimated by the Eq. (5), where $\mathcal{X}'_{\setminus \Omega}$ denotes predictive missing entries.

$$p(\Theta|\mathcal{X}'_{\Omega}) = \frac{p(\Theta, \mathcal{X}'_{\Omega})}{\int p(\Theta, \mathcal{X}'_{\Omega})d\Theta}$$
(4)

$$p(\mathcal{X}'_{\backslash\Omega}|\mathcal{X}'_{\Omega}) = \int p(\mathcal{X}'_{\backslash\Omega}|\Theta)p(\Theta,\mathcal{X}'_{\Omega})d\Theta \tag{5}$$

The exact Bayesian inference in (4) and (5) integrate over all latent variables and hyperparameters, which is analytically intractable. Therefore, a deterministic approximate inference under variational Bayesian (VB) framework is developed to learn the probabilistic CP factorization model [16]. Basically, a distribution $q(\Theta)$ based on the Eq. (4) and (5), is incorporated to approximate true posterior distribution $p(\Theta|X_l')$ by minimizing Kullback–Leibler (KL) divergence, which is denoted in the Eq. (6).

$$KL(q(\Theta)||p(\Theta|\mathcal{X}'_{\Omega}))$$
 (6)

The lower bound of Eq. (6) is solved by Eq. (7) and the maximum lower bound can be determined when KL divergence vanishes assuming $q(\Theta) = p(\Theta|\mathcal{X}'_{\Omega})$.

$$\mathcal{L}(q) = \int q(\Theta) \ln \left\{ \frac{p(\mathcal{X}'_{\Omega}, \Theta)}{q(\Theta)} \right\} d\Theta \tag{7}$$

Basically, for model learning via Bayesian inference, Eq. (6) is further leveraged to obtain the posterior distribution of the factor matrices, hyperparameters and lower bound of the model evidence. Moreover, during Bayesian inference-based model learning, tensor rank is determined automatically and implicitly updating λ in each iteration [16]. Specifically, the **Algorithm 1** adopted from [16], which is illustrated in Fig. 4. This algorithm can effectively correlate the latent multi-linear factors leveraging Bayesian inference based on the observed

data with a low-rank determination and also estimates the predictive distributions among missing entries. To avoid Bayesian inference to local minima, the initial points of the hyperparameter set are to a fixed value. After completion of the missing entries, the evaluation of missing data imputation can be quantified considering actual time-domain tensor $\mathcal{X}_{\Omega}(l)$ and estimated tensor $\widetilde{\mathcal{X}}_{\Omega}'(l)$, where the evaluation metric can be defined as relative standard error (RSE) in the Eq. (8).

$$RSE_{l} = \frac{\left\|\widetilde{\mathcal{X}}_{\Omega}'(l) - \mathcal{X}_{\Omega}(l)\right\|_{F}}{\left\|\mathcal{X}_{\Omega}(l)\right\|_{F}}$$
(8)

Algorithm 1: Fully Bayesian CP Factorization for tensor completion adapted from [16]

Input: A set of acoustics and vibration signals of missing entries with incomplete tensor $\{\mathcal{X}'_{\Omega}(l) \in \mathbb{R}^{D \times k}, l = 1, 2, ..., m\}$, where m is total number of observations.

Initialization: Initialization of hyperparameters $\boldsymbol{\Theta}$ set to fixed.

Output: Estimated tensor $\widetilde{\mathcal{X}}'_{\Omega}(l)$

Algorithm:

Step 1 (Estimated tensor calculation):

Repeat

For l = 1 : m

Calculate estimated tensor $\widetilde{\mathcal{X}}'_{\Omega}(l)$ leveraging Eq. (1)

enc

Reduce rank R by eliminating components of $\{\mathbf{X}^{(n)}\}$

Evaluate the lower bound using the Eq. (7)

until maximum number of iterations

Step 2 (evaluation of missing data imputation)

Relative standard error calculation from the Eq. (8)

Fig. 4. Fully Bayesian CP factorization algorithm.

Based on the **Algorithm 1**, the tensor rank can be determined automatically and in practice R is set manually for computational purpose. In this entire process λ updates in each iteration that results in a new prior over $\{X^{(n)}\}$ and then $\{X^{(n)}\}$ updates by using the new prior in the subsequent iteration.

4. Case study

The evaluation study was conducted on a testbed using a machinery faults simulator (MFS) manufactured by Spectra Quest Inc., which is illustrated in Fig. 3 [58] and equipped with multiple vibrations (accelerometers) and acoustics



Fig. 3. The MFS setup for data collection with acoustics and vibration sensors.

(microphones) sensors for real-time sensor signal acquisition purpose. Fig. 5 demonstrates accelerometers and microphone allocation in the MFS [58]. Sensor missing signals are generated as planned continuous missing based on the concept of a blackout situation. Equal channels of acoustics and vibration signals are unified, forming tensorial arrays, and a certain percentage of continuous missing signal scenarios is generated among different channels. It is worth noting that continuous missing entries is introduced at a random location with a varying missing percent based on a given length of signals, such as 1%, 3%, 5%, 10%, and 20% missing. Missing entries are imputed along with incomplete tensor completion by the FBCP method, which is illustrated in section 3.2. Finally, the performance of the estimated tensor $\widetilde{\mathcal{X}}'_{\Omega}(l)$ with missing completion was evaluated comparing with the actual tensor $\mathcal{X}_{0}(l)$.

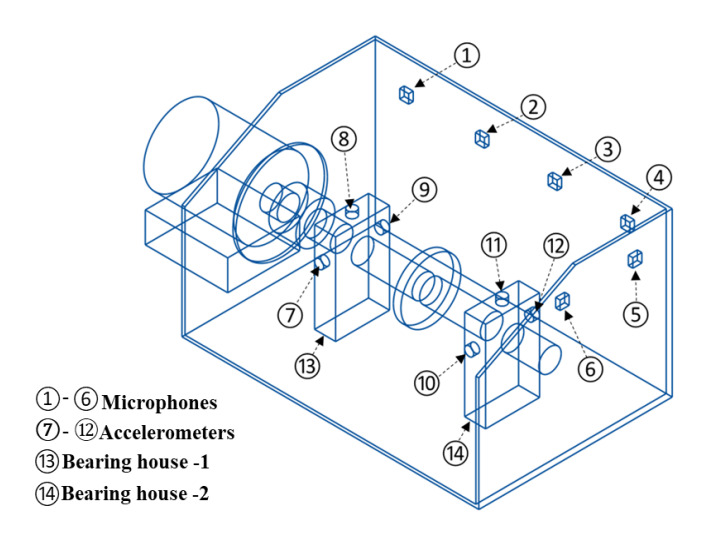


Fig. 5. Multi-channel sensor allocation in the MFS.

4.1. Experimental setup and data collection

In this study, acoustics and vibration signals were compiled by microphones and accelerometers, respectively. Adafruit® silicon MEMS microphones (SPW 2430 model) were incorporated for acoustic signal collection. Single-axis accelerometers (Industrial ICP® 608A11) were used for vibration signal acquisition. Sensitivity performance of accelerometer is 100 mV/g with the frequency ranges of 0.20 to 15 kHz. Six accelerometers were attached on the two bearing housings, where three accelerometers placed on each bearing house, respectively. These six accelerometers were connected to a data acquisition system for data collection with the sampling rate of 10,240 Hz. Also, six microphones were also embedded to the inside wall of the MFS chamber and connected to another data acquisition system to capture realtime acoustic emission signals at the sampling frequency of 8,000 Hz. The working motor speed was 30 Hz. Table 2 demonstrates the experimental design for five different bearing fault operating conditions and their corresponding observation numbers. The multi-channel sensor signals were collected after the motor reached the steady state operation conditions.

Table 2. Operation conditions performed in data collection.

Bearing house - 1	Bearing house - 2	Class label	Number of observations
Good	Good	1	12
Good	Ball fault	2	6
Ball fault	Good	2	6
Good	Inner race fault	3	6
Inner race fault	Good	3	6
Good	Outer race fault	4	6
Outer race fault	Good	4	6
Good	Combined fault	5	6
Combined fault	Good	5	6
Total			60

4.2. Missing data imputation and performance evaluation

In this study, planned missing signal is generated in timedomain tensor with 1%, 3%, 5%, 10%, and 20% percentage of continuous missing among different channels by considering each bearing fault conditions. Missing entries with timedomain tensor size is $12 \times 500 \times 12$, where 12, 500, and 12 represent the total number of channels, signal length, and number of observations for each bearing fault conditions, respectively. Continuous missing is calculated based on the length of signals, where 10% continuous missing equivalent to 50 lengths of continuous missing, which is generated among four different channels at different location randomly. The similar approach is also applicable when 20% missing equivalent to 100 lengths of continuous missing. In the given incomplete tensor size of $12 \times 500 \times 12$ is computed to estimated tensor using each observation starting from 1 to 12. Table 3 shows tuning parameters for FBCP-based tensor completion work. While each observation is iterated to 1 to 150 based on performance loss objective value of tolerance limit, which is set as 10^{-12} . In this incomplete-tensor completion, CP rank R = 15 is used. The performance evaluation of incomplete-tensor completion (estimated tensor), which is denoted by $\widetilde{\mathcal{X}}'_{\Omega}(l)$ is compared with the actual tensor $\mathcal{X}_{\Omega}(l)$. RSE is computed by the Eq. (8). It is worth noting that, tensor completion work is computationally faster when the tensor size is substantially small. To evaluate the effectiveness of the FBCP method, CP weighted optimization (CPWOPT) method is leveraged as benchmark method [50]. In the benchmark method CP rank R and number of iterations set to 15 and 150, respectively, which is similar to the FBCP method.

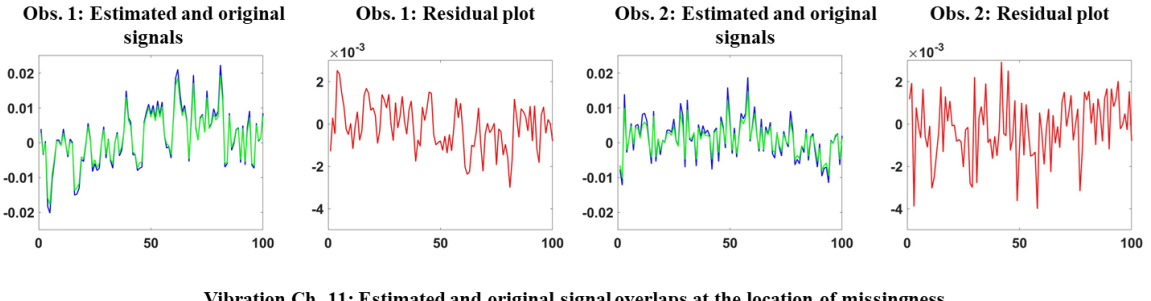
Table 3. Tuning parameter for FBCP-based tensor completion.

Tuning parameter	Value
CP Rank R	15
Tolerance limit	10^{-12}
Initial hyperparameter value	10^{-8}
Number of iterations	150

4.3. Results and discussion

Table 4 summarizes the performance of proposed and benchmark methods for the evaluation of estimated tensors based on channel-wise continuous missing percentages with five different bearing fault conditions and their respective RSE values. In different bearing conditions, channel-wise average RSE values are compared given corresponding missing

percentages at channel 1, 5, 9 and 11, where channel 1 and 5 corresponds to acoustics signals and channel 9 and 11 contain vibration signals. It is notable to mention that when a varying percentage of continuous missing signal scenarios are introduced at channel 1 then rest of 11 channels remained unchanged. Similar approaches are also applied in channels 5, 9 and 11 respectively. Fig. 6 demonstrates the performance of estimated signals at the location of missing occurrences (20% missing) and compares with the actual signals among acoustics and vibration channels. In acoustics channel-1, observations 1 and 2 show that estimated signals overlap the actual signals at the location of missing. Their residual plots show the effectiveness of the difference between estimated and actual signals. Similarly, at vibration channel 11, estimated signals overlap the actual at the location of a higher missing percentage (20% missing), and their residual plots show the effectiveness of estimated and actual signals. Fig. 7 shows an overall trend of RSE value in proposed and benchmark methods with respect to different missing percentages among five different bearing fault conditions. In contrast, it is noticeable that the proposed method performs better than the benchmark method with higher percentages of missing entries. Overall, the proposed method enables to capture the multi-linear latent factors among different channels with observed signals to impute continuous missing entries with substantially higher missing percentages. This proposed method was computed using the Intel (R) Core (TM) i9-12900 CPU @ 2.40 GHz.



Vibration Ch. 11: Estimated and original signal overlaps at the location of missingness

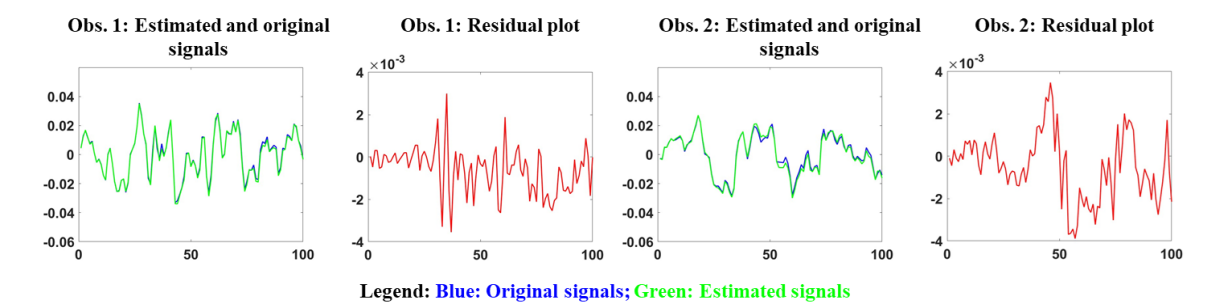


Fig. 6. Imputation of missing signals at the location of missing occurrences in acoustics and vibration channels (MP: 20%) with FBCP method.

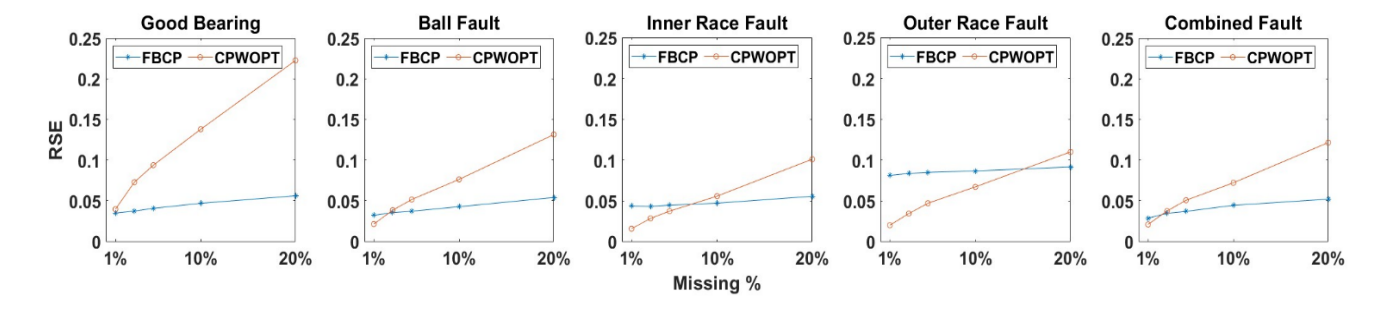


Fig. 7. Performance evaluation of proposed and benchmark methods with diverse bearing fault conditions.

MP: 1 % MP: 3 % MP: 5 % MP: 10 % MP: 20 % Bearing Avg. RSE Avg. RSE Avg. RSE Avg. RSE Ch. # Avg. RSE conditions CPWOPT FBCP CPWOPT FBCP CPWOPT FBCP **FBCP CPWOPT CPWOPT FBCP** Ch. 1 0.0358 0.0443 0.04060.0821 0.0453 0.10640.0500 0.1601 0.0582 0.2449 0.0357 0.0334 0.0392 0.0675 0.0830 0.0601 0.0825 0.1856 Ch. 5 0.0467 0.1126 Good bearing Ch. 9 0.0339 0.0470 0.0350 0.0879 0.0361 0.1115 0.0383 0.1595 0.0408 0.2460 0.0337 0.0339 0.0536 0.0343 0.0739 0.0388 0.2137 Ch.11 0.0331 0.1192 0.0423 0.0348 0.0372 0.0937 0.0468 0.1379 0.0560 0.2226 0.0395 0.0728 0.0406 Avg. 0.0347 0.0260 0.0402 0.0450 0.0419 0.0624 0.0889 0.1415 Ch. 1 0.0511 0.0644 Ch. 5 0.0351 0.0215 0.0429 0.03820.0469 0.0476 0.0590 0.0720 0.0806 0.1159 Ball fault Ch. 9 0.0280 0.0216 0.0280 0.0441 0.0286 0.0583 0.0293 0.0860 0.0362 0.1556 Ch.11 0.03030.0155 0.0302 0.02580.03080.0371 0.03100.0579 0.0347 0.11260.0320 0.0212 0.0353 0.0383 0.0370 0.0514 0.0426 0.0762 0.0539 Avg. 0.1314 0.0445 Ch. 1 0.0462 0.0175 0.0287 0.0437 0.0358 0.0508 0.0539 0.0519 0.0834 0.0420 0.0131 0.0434 0.0220 0.0463 0.0284 0.0470 0.0443 0.0560 0.0690 Ch. 5 Inner race fault Ch. 9 0.0468 0.0196 0.0452 0.03720.0464 0.0502 0.0473 0.0730 0.0644 0.1407 0.0397 0.0128 0.0400 0.0262 0.04250.0350 0.0439 0.0520 0.0500 0.1114 Ch.11 0.0158 Avg. 0.0437 0.0433 0.02850.0447 0.0374 0.0472 0.0558 0.0556 0.1011 0.0814 0.0828 0.0379 0.0843 0.0867 0.0729 0.0916 0.1159 Ch. 1 0.0228 0.0491 Ch. 5 0.0811 0.0192 0.0825 0.0305 0.0843 0.0391 0.0871 0.0566 0.0924 0.0866 Outer race fault Ch. 9 0.0223 0.0877 0.0430 0.0845 0.0896 0.0803 0.0924 0.1234 0.0819 0.0601 0.0807 0.0162 0.0814 0.0266 0.0872 0.0399 0.0831 0.0590 0.0899 0.1145 Ch.11 Avg. 0.0813 0.02010.08360.0345 0.08500.04710.0867 0.06720.0916 0.1101 Ch. 1 0.0299 0.0275 0.0343 0.0448 0.0379 0.0579 0.0461 0.0846 0.0597 0.1293 0.0322 0.0250 0.0406 0.0528 0.0753 Ch. 5 0.0372 0.0424 0.0553 0.0604 0.1117

0.0393

0.0246

0.0373

0.0272

0.0399

0.0368

0.0536

0.0350

0.0505

0.0288

0.0495

0.0443

Table 4 Summary results of proposed and benchmark method

5. Conclusion and future work

Ch. 9

Ch.11

Avg.

0.0262

0.0259

0.0285

0.0192

0.0116

0.0208

0.0265

0.0396

0.0344

Combined fault

The emerging trend of multi-channel sensor fusion is ubiquitous. In the industry 4.0 perspective, heterogeneous sensor fusion can be integrated for real-time machinery fault identification and diagnosis. Multi-channel sensor fusion can be challenging when a substantial amount of missing data occurrence prevails. However, the effectiveness of imputation of missing sensor signals is also significantly important for monitoring machinery conditions. In quest of the state-of-the-art, this proposed method adopted a fully Bayesian CANDECOMP/PARAFAC factorization (FBCP) method for missing data imputation from diverse bearing fault signals. To validate the effectiveness of this proposed method, a machinery fault simulator is used as a testbed to collect diverse bearing fault signals by integrating an equal number of acoustics (microphones) and vibration (accelerometers) sensors simultaneously. Acoustics and vibration signals are combined by forming time-domain tensors. A varying percentage of continuous missing signal scenarios are generated at random locations among different acoustics and vibration channels, constructing incomplete tensors. Then, the FBCP method is leveraged to complete the incomplete tensors and calculate estimated tensors. To evaluate the performance of continuous missing data imputation, relative standard errors (RSE) are computed based on the estimated and actual time-domain tensors. The weighted optimization (CPWOPT) method is incorporated as a benchmark method to evaluate the effectiveness of the FBCP method. Experimental results show that this proposed method can effectively impute a substantial portion of continuous missing data from diverse bearing fault scenarios.

For future work, this proposed method can be extended in the following aspects. Firstly, in real-world applications, multiple signal missing scenarios can occur to multiple acoustics and vibration channels simultaneously. The corresponding effectiveness of the FBCP method needs to be examined for this type of complex data missing scenarios. Secondly, this proposed method can be extended for bearing faults classification. More specifically, machine learning tools can be applied to the imputed multi-channel signals for bearing fault diagnosis, similar to the studies in [58].

0.0769

0.0513

0.0720

0.0313

0.0564

0.0519

0.1328

0.1122

0.1215

Acknowledgement

This work was partially sponsored by National Science Foundation CMMI-2046515.

References

- [1] J. Lee, B. Bagheri, and C. Jin, "Introduction to cyber manufacturing," *Manuf. Lett.*, vol. 8, pp. 11–15, 2016, doi: 10.1016/j.mfglet.2016.05.002.
- [2] J. Lee, B. Bagheri, and H. A. Kao, "A Cyber-Physical Systems architecture for Industry 4.0-based manufacturing systems," *Manuf. Lett.*, vol. 3, pp. 18–23, 2015, doi: 10.1016/j.mfglet.2014.12.001.
- [3] M. M. Herterich, F. Uebernickel, and W. Brenner, "The impact of cyber-physical systems on industrial services in manufacturing," *Procedia CIRP*, vol. 30, pp. 323–328, 2015, doi: 10.1016/j.procir.2015.02.110.
- [4] J. Lee, E. Lapira, B. Bagheri, and H. an Kao, "Recent advances and trends in predictive manufacturing systems in big data environment," *Manuf. Lett.*, vol. 1, no. 1, pp. 38–41, 2013, doi:

- 10.1016/j.mfglet.2013.09.005.
- [5] A. Diez-Olivan, J. Del Ser, D. Galar, and B. Sierra, "Data fusion and machine learning for industrial prognosis: Trends and perspectives towards Industry 4.0," *Inf. Fusion*, vol. 50, no. October 2018, pp. 92–111, Oct. 2019, doi: 10.1016/j.inffus.2018.10.005.
- [6] Y. LI, X. DU, F. WAN, X. WANG, and H. YU, "Rotating machinery fault diagnosis based on convolutional neural network and infrared thermal imaging," *Chinese J. Aeronaut.*, vol. 33, no. 2, pp. 427–438, Feb. 2020, doi: 10.1016/j.cja.2019.08.014.
- [7] N. Tandon and B. C. Nakra, "Comparison of vibration and acoustic measurement techniques for the condition monitoring of rolling element bearings," *Tribol. Int.*, vol. 25, no. 3, pp. 205– 212, 1992, doi: 10.1016/0301-679X(92)90050-W.
- [8] N. Baydar and A. Ball, "Detection of gear failures via vibration and acoustic signals using wavelet transform," *Mech. Syst. Signal Process.*, vol. 17, no. 4, pp. 787–804, 2003, doi: 10.1006/mssp.2001.1435.
- [9] P. Henriquez, J. B. Alonso, M. A. Ferrer, and C. M. Travieso, "Review of automatic fault diagnosis systems using audio and vibration signals," *IEEE Trans. Syst. Man, Cybern. Syst.*, vol. 44, no. 5, pp. 642–652, 2014, doi: 10.1109/TSMCC.2013.2257752.
- [10] M. Zhao, Y. Li, S. Chen, and B. Li, "Missing value recovery for encoder signals using improved low-rank approximation," *Mech. Syst. Signal Process.*, vol. 139, p. 106595, May 2020, doi: 10.1016/j.ymssp.2019.106595.
- [11] Q. Ma, Y. Gu, W.-C. Lee, and G. Yu, "Order-Sensitive Imputation for Clustered Missing Values (Extended Abstract)," in 2019 IEEE 35th International Conference on Data Engineering (ICDE), Apr. 2019, vol. 2019-April, no. 1, pp. 2147–2148. doi: 10.1109/ICDE.2019.00268.
- [12] J. Zhu, Z. Ge, Z. Song, and F. Gao, "Review and big data perspectives on robust data mining approaches for industrial process modeling with outliers and missing data," *Annu. Rev. Control*, vol. 46, pp. 107–133, 2018, doi: 10.1016/j.arcontrol.2018.09.003.
- [13] Y. Li *et al.*, "A large-scale sensor missing data imputation framework for dams using deep learning and transfer learning strategy," *Measurement*, vol. 178, no. April, p. 109377, Jun. 2021, doi: 10.1016/j.measurement.2021.109377.
- [14] P. Bansal, P. Deshpande, and S. Sarawagi, "Missing value imputation on multidimensional time series," *Proc. VLDB Endow.*, vol. 14, no. 11, pp. 2533–2545, Jul. 2021, doi: 10.14778/3476249.3476300.
- [15] X. Chen, M. Lei, N. Saunier, and L. Sun, "Low-Rank Autoregressive Tensor Completion for Spatiotemporal Traffic Data Imputation," *IEEE Trans. Intell. Transp. Syst.*, vol. 23, no. 8, pp. 12301–12310, 2022, doi: 10.1109/TITS.2021.3113608.
- [16] Q. Zhao, L. Zhang, and A. Cichocki, "Bayesian CP factorization of incomplete tensors with automatic rank determination," *IEEE Trans. Pattern Anal. Mach. Intell.*, vol. 37, no. 9, pp. 1751–1763, 2015, doi: 10.1109/TPAMI.2015.2392756.
- [17] C. K. Enders, "Listwise Deletion," in *Dictionary of Statistics & Methodology*, 2455 Teller Road, Thousand Oaks California 91320 United States of America: SAGE Publications, Inc., 2005. doi: 10.4135/9781412983907.n1075.
- [18] A. M. Sefidian and N. Daneshpour, "Missing value imputation using a novel grey based fuzzy c-means, mutual information based feature selection, and regression model," *Expert Syst.*

- *Appl.*, vol. 115, pp. 68–94, Jan. 2019, doi: 10.1016/j.eswa.2018.07.057.
- [19] T. Canchala-Nastar, Y. Carvajal-Escobar, W. Alfonso-Morales, W. Loaiza Cerón, and E. Caicedo, "Estimation of missing data of monthly rainfall in southwestern Colombia using artificial neural networks," *Data Br.*, vol. 26, p. 104517, Oct. 2019, doi: 10.1016/j.dib.2019.104517.
- [20] A. Z. Alruhaymi and C. J. Kim, "Study on the Missing Data Mechanisms and Imputation Methods," *Open J. Stat.*, vol. 11, no. 04, pp. 477–492, 2021, doi: 10.4236/ojs.2021.114030.
- [21] D. B. RUBIN, "Inference and missing data," *Biometrika*, vol. 63, no. 3, pp. 581–592, 1976, doi: 10.1093/biomet/63.3.581.
- [22] A. N. Baraldi and C. K. Enders, "An introduction to modern missing data analyses," *J. Sch. Psychol.*, vol. 48, no. 1, pp. 5–37, 2010, doi: 10.1016/j.jsp.2009.10.001.
- [23] E. Javanmardi, Y. Gu, M. Javanmardi, and S. Kamijo, "Autonomous vehicle self-localization based on abstract map and multi-channel LiDAR in urban area," *IATSS Res.*, vol. 43, no. 1, pp. 1–13, 2019, doi: 10.1016/j.iatssr.2018.05.001.
- [24] M. M. Nabi, V. Senyurek, A. C. Gurbuz, and M. Kurum, "Deep Learning-Based Soil Moisture Retrieval in CONUS Using CYGNSS Delay Doppler Maps," *IEEE J. Sel. Top. Appl. Earth Obs. Remote Sens.*, vol. 15, pp. 6867–6881, 2022, doi: 10.1109/JSTARS.2022.3196658.
- [25] A. Senanayaka et al., "Similarity-based Multi-source Transfer Learning Approach for Time Series Classification," Int. J. Progn. Heal. Manag., vol. 13, no. 2, pp. 1–25, Oct. 2022, doi: 10.36001/ijphm.2022.v13i2.3267.
- [26] C. Sun, Y. Chen, and C. Cheng, "Imputation of missing data from offshore wind farms using spatio-temporal correlation and feature correlation," *Energy*, vol. 229, p. 120777, Aug. 2021, doi: 10.1016/j.energy.2021.120777.
- [27] M. Martinez-Luengo, M. Shafiee, and A. Kolios, "Data management for structural integrity assessment of offshore wind turbine support structures: data cleansing and missing data imputation," *Ocean Eng.*, vol. 173, no. November 2018, pp. 867–883, Feb. 2019, doi: 10.1016/j.oceaneng.2019.01.003.
- [28] L. Pan and J. Li, "K-Nearest Neighbor Based Missing Data Estimation Algorithm in Wireless Sensor Networks," Wirel. Sens. Netw., vol. 02, no. 02, pp. 115–122, 2010, doi: 10.4236/wsn.2010.22016.
- [29] A. L. Hartzell, M. G. da Silva, and H. R. Shea, *MEMS Reliability*. Boston, MA: Springer US, 2011. doi: 10.1007/978-1-4419-6018-4.
- [30] S. Razza and S. Burdo, "An underestimated issue: unsuspected decrease of sound processor microphone sensitivity, technical, and clinical evaluation," *Cochlear Implants Int.*, vol. 12, no. 2, pp. 114–123, May 2011, doi: 10.1179/146701010X486499.
- [31] R. Vasta, I. Crandell, A. Millican, L. House, and E. Smith, "Outlier detection for sensor systems (ODSS): A MATLAB macro for evaluating microphone sensor data quality," *Sensors* (Switzerland), vol. 17, no. 10, 2017, doi: 10.3390/s17102329.
- [32] E. L. Silva-Ramírez, R. Pino-Mejías, M. López-Coello, and M. D. Cubiles-de-la-Vega, "Missing value imputation on missing completely at random data using multilayer perceptrons," *Neural Networks*, vol. 24, no. 1, pp. 121–129, 2011, doi: 10.1016/j.neunet.2010.09.008.
- [33] P. J. García-Laencina, J.-L. Sancho-Gómez, A. R. Figueiras-Vidal, and M. Verleysen, "K nearest neighbours with mutual

- information for simultaneous classification and missing data imputation," *Neurocomputing*, vol. 72, no. 7–9, pp. 1483–1493, Mar. 2009, doi: 10.1016/j.neucom.2008.11.026.
- [34] D. M. P. Murti, U. Pujianto, A. P. Wibawa, and M. I. Akbar, "K-Nearest Neighbor (K-NN) based Missing Data Imputation," in 2019 5th International Conference on Science in Information Technology (ICSITech), Oct. 2019, pp. 83–88. doi: 10.1109/ICSITech46713.2019.8987530.
- [35] J. Maillo, S. Ramírez, I. Triguero, and F. Herrera, "kNN-IS: An Iterative Spark-based design of the k-Nearest Neighbors classifier for big data," *Knowledge-Based Syst.*, vol. 117, pp. 3– 15, Feb. 2017, doi: 10.1016/j.knosys.2016.06.012.
- [36] E. Acuña and C. Rodriguez, "The Treatment of Missing Values and its Effect on Classifier Accuracy," in *Classification*, *Clustering, and Data Mining Applications*, no. 1995, Berlin, Heidelberg: Springer Berlin Heidelberg, 2004, pp. 639–647. doi: 10.1007/978-3-642-17103-1 60.
- [37] S. Zhang, J. Zhang, X. Zhu, Y. Qin, and C. Zhang, "Missing Value Imputation Based on Data Clustering," *Trans. Comput. Sci. I*, no. 60625204, pp. 128–138, 2008, doi: 10.1007/978-3-540-79299-4-7.
- [38] Z. Che, S. Purushotham, K. Cho, D. Sontag, and Y. Liu, "Recurrent Neural Networks for Multivariate Time Series with Missing Values," *Sci. Rep.*, vol. 8, no. 1, p. 6085, Dec. 2018, doi: 10.1038/s41598-018-24271-9.
- [39] J. Yoon, W. R. Zame, and M. van der Schaar, "Estimating Missing Data in Temporal Data Streams Using Multi-directional Recurrent Neural Networks," *IEEE Trans. Biomed. Eng.*, vol. 66, no. 5, pp. 1477–1490, Nov. 2017, doi: 10.1109/TBME.2018.2874712.
- [40] Y. Peng, W. Qiao, and L. Qu, "Compressive Sensing-Based Missing-Data-Tolerant Fault Detection for Remote Condition Monitoring of Wind Turbines," *IEEE Trans. Ind. Electron.*, vol. 69, no. 2, pp. 1937–1947, Feb. 2022, doi: 10.1109/TIE.2021.3057039.
- [41] D. Craven, B. McGinley, L. Kilmartin, M. Glavin, and E. Jones, "Compressed sensing for bioelectric signals: A review," *IEEE J. Biomed. Heal. Informatics*, vol. 19, no. 2, pp. 529–540, 2015, doi: 10.1109/JBHI.2014.2327194.
- [42] Y. Nan, Z. Yi, and C. Bingxia, "Review of compressed sensing for biomedical imaging," *Proc. 2015 7th Int. Conf. Inf. Technol. Med. Educ. ITME 2015*, pp. 225–228, 2016, doi: 10.1109/ITME.2015.119.
- [43] T. G. Kolda and B. W. Bader, "Tensor decompositions and applications," SIAM Rev., vol. 51, no. 3, pp. 455–500, 2009, doi: 10.1137/07070111X.
- [44] E. E. Papalexakis, C. Faloutsos, and N. D. Sidiropoulos, "Tensors for data mining and data fusion: Models, applications, and scalable algorithms," *ACM Trans. Intell. Syst. Technol.*, vol. 8, no. 2, 2016, doi: 10.1145/2915921.
- [45] F. L. Hitchcock, "The Expression of a Tensor or a Polyadic as a Sum of Products," *J. Math. Phys.*, vol. 6, no. 1–4, pp. 164–189, Apr. 1927, doi: 10.1002/sapm192761164.
- [46] J. D. Carroll and J.-J. Chang, "Analysis of individual differences in multidimensional scaling via an n-way generalization of

- 'Eckart-Young' decomposition," *Psychometrika*, vol. 35, no. 3, pp. 283–319, Sep. 1970, doi: 10.1007/BF02310791.
- [47] R. a Harshman, "Foundations of the PARAFAC procedure: Models and conditions for an 'explanatory' multimodal factor analysis," *UCLA Work. Pap. Phonetics*, vol. 16, no. 10, pp. 1– 84, 1970.
- [48] Q. Song, H. Ge, J. Caverlee, and X. Hu, "Tensor Completion Algorithms in Big Data Analytics," ACM Trans. Knowl. Discov. Data, vol. 13, no. 1, pp. 1–48, Jan. 2019, doi: 10.1145/3278607.
- [49] H. Lu, K. N. Plataniotis, and A. N. Venetsanopoulos, "MPCA: Multilinear principal component analysis of tensor objects," *IEEE Trans. Neural Networks*, 2008, doi: 10.1109/TNN.2007.901277.
- [50] E. Acar, D. M. Dunlavy, T. G. Kolda, and M. Mørup, "Scalable tensor factorizations for incomplete data," *Chemom. Intell. Lab. Syst.*, vol. 106, no. 1, pp. 41–56, Mar. 2011, doi: 10.1016/j.chemolab.2010.08.004.
- [51] L. Sorber, M. Van Barel, and L. De Lathauwer, "Optimization-based algorithms for tensor decompositions: Canonical polyadic decomposition, decomposition in rank-(Lr, Lr, 1) terms, and a new generalization," SIAM J. Optim., vol. 23, no. 2, pp. 695–720, Jan. 2013, doi: 10.1137/120868323.
- [52] H. Kasai and B. Mishra, "Riemannian preconditioning for tensor completion," 33rd Int. Conf. Mach. Learn., no. Icml, pp. 1–20, Jun. 2015.
- [53] Ji Liu, P. Musialski, P. Wonka, and Jieping Ye, "Tensor completion for estimating missing values in visual data," in 2009 IEEE 12th International Conference on Computer Vision, Sep. 2009, vol. 35, no. 1, pp. 2114–2121. doi: 10.1109/ICCV.2009.5459463.
- [54] L. Xiong, X. Chen, T.-K. Huang, J. Schneider, and J. G. Carbonell, "Temporal Collaborative Filtering with Bayesian Probabilistic Tensor Factorization," in *Proceedings of the 2010 SIAM International Conference on Data Mining*, Apr. 2010, pp. 211–222. doi: 10.1137/1.9781611972801.19.
- [55] J. Håstad, "Tensor rank is NP-complete," in Lecture Notes in Computer Science (including subseries Lecture Notes in Artificial Intelligence and Lecture Notes in Bioinformatics), vol. 372 LNCS, 1989, pp. 451–460. doi: 10.1007/BFb0035776.
- [56] X. Chen, Z. He, and L. Sun, "A Bayesian tensor decomposition approach for spatiotemporal traffic data imputation," *Transp. Res. Part C Emerg. Technol.*, vol. 98, no. June 2018, pp. 73–84, 2019, doi: 10.1016/j.trc.2018.11.003.
- [57] T. G. Kolda and B. W. Bader, "Tensor Decompositions and Applications," *SIAM Rev.*, vol. 51, no. 3, pp. 455–500, Aug. 2009, doi: 10.1137/07070111X.
- [58] A. Al Mamun *et al.*, "Multi-channel sensor fusion for real-time bearing fault diagnosis by frequency-domain multilinear principal component analysis," *Int. J. Adv. Manuf. Technol.*, pp. 1–14, 2022.